The Gramicidin Pore: Crystal Structure of a Cesium Complex

B. A. WALLACE AND K. RAVIKUMAR

Gramicidin, a linear polypeptide composed of hydrophobic amino acids with alternating L- and D- configurations, forms transmembrane ion channels. The crystal structure of a gramicidin-cesium complex has been determined at 2.0 angstrom resolution. In this structure, gramicidin forms a 26 angstrom long tube comprised of two polypeptide chains arranged as antiparallel beta strands that are wrapped into a left-handed helical coil with 6.4 residues per turn. The polypeptide backbone forms the interior of the hydrophilic, solvent-filled pore and the side chains form a hydrophobic and relatively regular surface on the outside of the pore. This example of a crystal structure of a solvent-filled ion pore provides a basis for understanding the physical nature of ion translocation.

THE TRANSPORT OF IONS ACROSS BIOLOGICAL MEMBRANES is mediated by channels. These molecules act to facilitate diffusion of hydrophilic molecules across the hydrophobic barrier of the phospholipid bilayer. Gramicidin A is the best characterized ion channel in terms of its conductance properties and the observed effects of alterations in amino acid side chains on its transport properties (*1*). It permits passive diffusion of monovalent cations with diameters of up to ~5 Å. Gramicidin is a linear polypeptide consisting of 16 residues, 15 of which are amino acids. The COOH-terminal residue is an ethanolamine (a glycine with a methylene instead of a carbonyl group). The gramicidin sequence is (*2*):

Formyl-L-Val-Gly-L-Ala-D-Leu-L-Ala-D-Val-L-Val-D-Val-
L-Trp-D-Leu-L-Trp-D-Leu-L-Trp-D-Leu-L-Trp-ethanolamine

Alternating residues in the sequence have opposite chirality. The active form of the molecule is a dimer (*3*). This relatively small polypeptide is capable of adopting several different conformations, depending on its environment. Its two major conformers have been designated the "channel" and the "pore" structures. The channel corresponds to the predominant conducting form in membranes and appears to be an amino terminal–to–amino terminal helical dimer, similar to the type of structure originally proposed by Urry *et al.* (*4*). The orientation and general folding motif of the channel have been established by nuclear magnetic resonance (*5*), fluorescence (*6*), and conductance (*7*) measurements, among others. The pore apparently corresponds to the minor conducting form detected in black lipid membrane preparations, which has a very long mean channel lifetime. The pore is also the predominant form found in organic solutions, and is one of the family of antiparallel intertwined double helices first proposed for the gramicidin structure by Veatch *et al.* (*8*). The channel and pore forms are readily distinguished by their distinctly different circular dichroism spectra and by their differential responses to the binding of ions (*9, 10*).

Crystals of an unliganded form of gramicidin were first reported in 1949 (*11*). Later, several types of crystalline gramicidin-ion complexes were prepared (*10, 12–14*). The structures of all of these crystals have remained unsolved until now, because this molecule falls in the intermediate size range for which x-ray crystal structure determinations are difficult: the asymmetric units are generally too large for direct methods and are rather small for multiple isomorphous replacement methods. The problems in the latter case stem from the low solvent content of the crystals, the extreme sensitivity of the structure to environmental changes that produce nonisomorphism, and the lack of appropriate side chains for heavy-atom derivatization. To overcome these problems, we have used a phasing method that does not rely on the production of isomorphous derivatives, that of single wavelength anomalous scattering. This method uses the Bijvoet differences produced by an anomalous scatterer and the partial structure of that scatterer to determine the phases in a single crystal (*15*). In this case, we have incorporated cesium into the crystal to act as the anomalous scatterer. The use of cesium has the additional benefit that, because cesium ions are transported by gramicidin, the crystals formed provide a view of the pore structure in complex with its ligand. We have previously reported the initial phasing of the gramicidin-cesium crystals and tracing of the polypeptide chains (*10, 16*); here we describe the details of the high-resolution structure of the gramicidin-cesium complex.

Crystallization and structure determination. Gramicidin A (25 mg/ml) was crystallized from a 63 m*M* solution of CsCl in methanol (*10*). The crystals formed are lenticular and are of the orthorhombic space group $P2_12_12_1$, with unit cell dimensions a = 31.11 Å, b = 52.10 Å, and c = 32.17 Å.

X-ray data to a maximum resolution of 1.8 Å were collected with a Picker FACS-1 diffractometer. Friedel pairs were treated independently during data reduction. Structure factors for the individual Friedel mates were included throughout the refinement because of the large partial structure of the anomalous scatterer (Table 1) (*17*).

The preliminary positions of the cesiums were determined from difference Patterson maps calculated with coefficients of $(\Delta F)^2$, where $\Delta F = |F(h)| - |F(-h)|$. A molecular model was built based on the 1.8 Å resolution electron density map (Fig. 1). Details of the data collection and phase determination have been described (*10, 16, 17*). Atomic coordinates and temperature factors were subjected to a series of cycles of stereochemically restrained least-squares refine-

B. A. Wallace is a professor and K. Ravikumar is a postdoctoral associate in the Department of Chemistry and Center for Biophysics, Rensselaer Polytechnic Institute, Troy, NY 12180.

Table 1. Statistics for structure determination.

Bijovet difference ($\langle\|\Delta F\|\rangle/\langle F_p\rangle$) (percent)	8.8
Partial structure of cesium ($\langle F_A\rangle/\langle F_p\rangle$) (percent)	43
Number of reflections $\geq 3\sigma$	3317
Number of atoms (non-hydrogen)	596
Number of solvents located	38
R factor	0.226
Average *B* value (Å^2)	14.85
Deviations (rms)	
Bond distance (Å)	0.016
From planarity (Å)	0.015

Table 2. Intradimer hydrogen bonds in the gramicidin pore.

N4 ...036*	N24...016*	N1 ...033†	N21...013†
N6 ...034*	N26...014*	N3 ...031†	N23...011†
N8 ...032*	N28...012*	N5 ...029†	N25...09†
N10...030*	N30...010*	N7 ...027†	N27...07†
N12...028*	N32...08*	N9 ...025†	N29...05†
N14...026*	N34...06*	N11...023†	N31...03†
N16...024*	N36...04*	N13...021†	N33...01†

*Indicates a hydrogen bond formed by the superhelical twist of the β sheet. †Indicates a hydrogen bond formed within the antiparallel β sheet motif.

ment (*18*) with the use of a dictionary updated with D-amino acids and with the chiral restraints disabled, alternating with manual refittings of the model to the electron density made with the molecular model-building program FRODO (*19*). In the initial map, it appeared that the hydrogen bonds of the pore might be of somewhat different lengths than those typically found in soluble proteins. Hence, this parameter was not restrained in the stereochemical refinement. The current *R* factor at 2.0 Å resolution is 0.226. Every backbone and side chain atom in the structure has been located. In addition, 38 solvent sites have presently been identified and refined at full occupancy. The resulting structure is sufficiently reliable to allow us to describe it in atomic detail. Statistics for the refinement are given in Table 1. Coordinates of the refined gramicidin-cesium complex will be deposited at the Brookhaven Protein Data Bank.

Molecular conformation of the gramicidin pore. The gramicidin-cesium complex crystallizes with two gramicidin dimers per asymmetric unit (Fig. 2). The dimers are tube-like structures that are approximately 26 Å in length. Each dimer is a left-handed double helix comprised of two antiparallel polypeptide chains with a β sheet-type hydrogen-bonding pattern. The folding of the polypeptides may be envisioned as two β strands (one from each polypeptide) running antiparallel to each other and forming a symmetric sheet that is held together by fourteen interstrand hydrogen bonds (these bonds are denoted by a "†" in Table 2). Alternating (even-numbered) residues would have free amide and carbonyl groups located along the edges of the sheet. The sheet is then rolled up in the direction of the sheet axis to produce a helical structure (Fig. 3) to form an additional 14 hydrogen bonds (designated as "*" in Table 2) with the free sites on the other polypeptide chain. This structure leaves only two other potential hydrogen-bonding sites at each of the ends of the helix. All of the hydrogen bonds run nearly parallel to the axis of the helix; half of them point with their dipoles in one direction and half in the opposite direction. The helical twist is such that each polypeptide makes 2.5 complete turns and thus has a pitch of 6.4 residues per turn. This double helical motif has alternating strands along the helix from different polypeptide chains (seen as different colors in Fig. 4), so that, whereas the rise per turn for an individual polypeptide is 10.4 Å, the average helix strand separation along the axis is ~5.2 Å. The average hydrogen bond length along the backbone is 2.8 Å, but there is considerable and regular variation from this average value; the hydrogen bonds involving even-numbered residues have a shorter than average length (2.7 Å), and those involving odd-numbered residues have a longer than average length of 2.9 Å. Because the odd- and-even-numbered hydrogen bonds are paired between different turns of the helix, this results in a difference of about 0.2 Å in the average separation distances between alternating pairs of strands along the helix axis.

There is a "stagger" of three residues in the linear arrangement of polypeptides at each end of the sheet, where the amide of residue 1 of one chain forms a hydrogen bond with the carbonyl group of the 13th residue of the other chain, which leaves residues 14 through 16 unpaired within the sheet. Interestingly, when the sheet is rolled up, this stagger produces nearly flat surfaces at the ends of the pore, since residues 14 and 16 form hydrogen bonds with the adjacent strand. Only residues 2 and 15 are not hydrogen-bonded within the dimer.

The double helical folding motif produces a pore because of the stereochemical nature of the amino acids in the gramicidin sequence. Normally a β sheet formed of all L-amino acids would have side chains protruding alternately above and below the plane of the sheet. However, in gramicidin, which has alternating L- and D-amino acids, all side chains protrude on one side of the sheet. When the sheet is rolled up, the side chains (all of which are hydrophobic) are located on the exterior of the helix. The center of the helix is not blocked by side chains, and the hole formed can accommodate ions and solvent. The diameter of the hole is 4.9 Å (van der Waals–to–van der Waals), and hence it can easily accommodate ions. The polypeptide backbone provides a hydrophilic environment for the ions and solvent molecules inside the pore.

The hydrophobic side chains are located at the periphery of the pore, in the region of the interface between dimers and surrounding

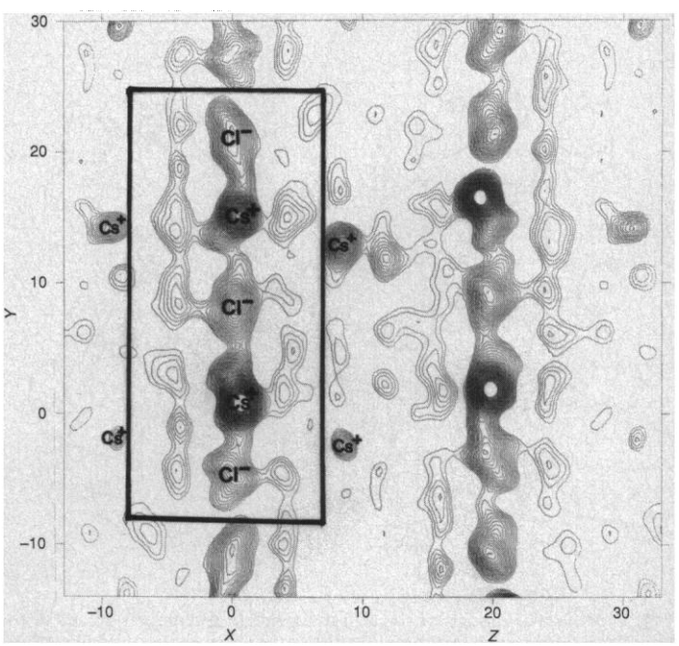

Fig. 1. Section (z = 10) of the initial 1.8 Å electron density map showing the location of the ions in the center of the pore. The box indicates the bounds of the polypeptide backbone of one of the dimers in the asymmetric unit. The other dimer is related to this by approximately a 16 Å translation in the x direction and a rotation of 180 degrees about y. The locations of the two cesium and three chloride ions in the pore are clearly seen, as are the two cesium sites located between dimers. The polypeptide backbone densities that merge with the cesium densities are from the carbonyl oxygens, which are displaced from the helix axis to form the binding sites for the cations.

hydrophobic solvent. Although most of the side chains are relatively bulky (tryptophans and leucines), they pack in a way that results in a relatively uniform outside diameter (~16 Å) along the length of the pore. The average X_2 angle for the tryptophans is ~90 degrees, which means that the aromatic rings are not oriented perpendicular to the helix axis, but more or less lie parallel to it. In general, the tryptophans interleave with average dihedral angles of ~75 degrees to produce a herringbone-type arrangement, as is often seen in soluble proteins (*20*).

Thus the double helical folding motif is a very simple and efficient use of polypeptide chain to create a hydrophilic cavity for ions and a hydrophobic surface for exposure to membrane hydrocarbon chains. A bundle of α helices would require five to six times as many residues to create a cavity of comparable size.

The ligand binding sites. Cesium and chloride ions, as well as solvent molecules, are located in the center of the pore. The presence of these ions provides us with an opportunity to examine pore-ligand interactions. At first glance it would seem that, since the backbone is relatively homogeneous, the cesiums could occupy any number of sites with similar probabilities, as if the environment were uniform. This is not the case, however. At equilibrium in the crystal, there are two discrete sites in the pore where cesiums bind (at full occupancy). In each of these sites, there is some anisotropy (smearing of the density) of the ions in the γ direction (along the helix axis) (see Fig. 5). Although the polypeptide backbone does form a relatively uniform tube, we note that in the regions that form the ion binding sites, the backbone is somewhate distorted from its average ϕ, ψ angles. This distortion results in a slight puckering of the chain. In general, the carbonyl bonds lie parallel to the axis of the helix. However, several carbonyl groups nearest the cesiums are tilted in toward the center of the pore (by up to 40 degrees from the helix axis) to permit complexation. Although the position of the most anisotropic cesium is not as precisely defined as the others, the locations of the ions are in nearly symmetric positions with respect to the various polypeptide chains. For each cesium ion, the atoms that are generally closest are the carbonyl oxygens of the 11th and 14th residues of one polypeptide chain (the average cesium-oxygen distance is 3.6Å). Since these residues are separated by approximately one half turn of helix, they are located on opposite sides of the pore. The closest atoms in the other polypeptide chain are the carbonyl oxygens of residues 2 and 3, which are located at an average distance of 3.8 Å.

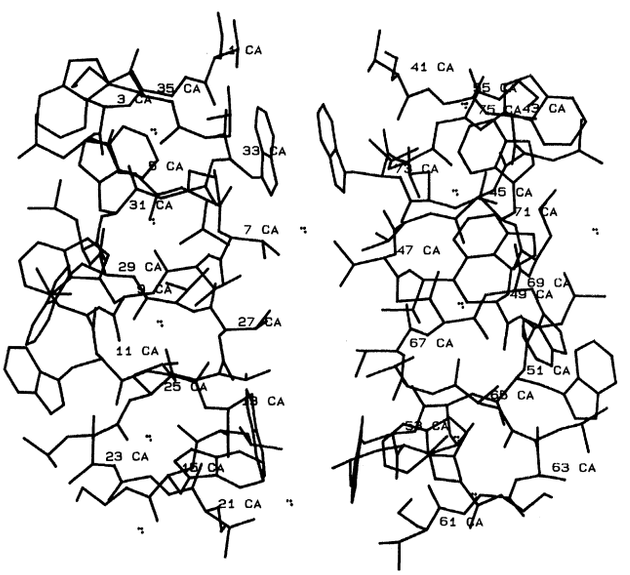

Fig. 2. Molecular models of the two independent gramicidin dimers in the crystallographic asymmetric unit. To distinguish between equivalent residues in the four different polypeptide chains, the residues in the two monomers on the left-hand side of the figures are numbered from 1 to 16 and from 21 to 36, and the monomers in the dimer on the right-hand side have been numbered from 41 to 56 and from 61 to 76. That is, val-1 will be designated as residue 1, 21, 41, or 61, depending on the monomer in which it is located. Although the backbone folds of all four monomers are similar, the side-chain conformations differ somewhat. There is more similarity between monomer 1 to 16 and monomer 41 to 56 than there is between monomers in the same dimer (that is, 1 to 16 and 21 to 36).

Fig. 3. Schematic diagram showing the backbone fold and hydrogen-bonding pattern present in the gramicidin pore structure.

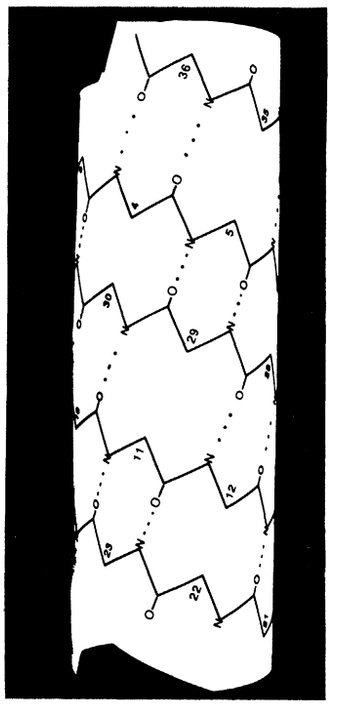

There are also three chloride ions in each pore. This finding was somewhate unexpected, since gramicidin is considered a cation transporter, although there has been some evidence for anion permeability and anion influence on cation permeability (*21*). Sung and Jordan (*22*) calculated that for the channel form of the molecule, the barrier to chloride binding is at the opening of the channel; if this barrier could be surmounted, the chlorides should be stable in the interior of the channel. The barriers in the pore form may be somewhat different. The observed presence of chlorides in the crystals may be a consequence of the relatively high salt concentration used to form the crystals. If this is the case, the chlorides may be occupying sites that would otherwise contain solvent molecules. The chloride positions are considerably more variable than the cesium positions with respect to the identity of adjacent residues in the polypeptide backbone. However, there are at least two amide nitrogen atoms within 4 Å of each of the chlorides. The distances between all cesiums and chlorides are >5 Å, which indicates they exist as individual ions. There are also a number of solvent molecules within the pore, between the ions, and especially at the ends of the pore. The precise positions and occupancies of all of the ordered solvent molecules should become apparent as the structure is further refined.

There are two "extra-pore" cesium sites that lie in the region between the dimers. Both of these sites are only partially occupied (one with an occupancy of 0.6 and the other with an occupancy of 0.4). Thus in the crystallographic asymmetric unit there is a precise 1:1 molar ratio of anions and cations, although there are a total of eight cesium and six chloride sites. The molar ratio of cesium to gramicidin dimer in these crystals is 3:1. The extra-pore cesium sites

are mostly surrounded by methanol molecules and may have a role in maintaining crystal stability. Since gramicidin has no hydrophilic side chains, the amino acid side chains that are nearest these cesiums are necessarily hydrophobic. Such residues include, for one cesium, the 14th residue from each dimer (Leu^{14} and Leu^{54}), and for the other cesium, the 13th residue from the other chain in each dimer (Trp^{33} and Trp^{73}). The two tryptophans are aligned with a dihedral angle of ~0 degrees, and this interaction may contribute to the crystal stability. The symmetric positions of the two dimers with respect to the cesium sites result from the noncrystallographic symmetry relation between dimers (see Fig. 1). The extra-pore cesiums appear to be somewhat less anisotropic than those located in the pore.

Similarities between dimers. The two dimers in the asymmetric unit adopt nearly identical structures. Furthermore, the structures of the two monomers within each dimer are also very similar. The correlation coefficient, which shows the correspondence of the scattering densities of the dimers, is 0.74, whereas the correlation coefficient between the two monomers in each dimer is 0.54. Thus the folds of all monomers are found to be similar, with the structures of corresponding monomers in different dimers (residues 1 to 16 and 41 to 56 in our numbering scheme) being nearly identical [the root-mean-square (rms) deviation for all of the atoms is 0.086 Å]; for the different monomers within the same dimer (that is, residues 1 to 16 versus 21 to 36) the rms deviation is 0.103 Å. Most of the differences in the structures are in the side chain conformations. When the density correlation is made at a lower radius (for example, including only backbone densities), it increases to 0.78. Furthermore, the average rms deviation between only backbone atoms is <0.04 Å, which suggests that these structures are quite similar. For that reason we have only discussed the structure of a single dimer in this article. That the major difference derives from the side chains is reasonable, since these are the parts of the structure that are at the interface between molecules. As such, they are subject to packing differences, especially those caused by the cesium ions outside the pores, which are located at nonsymmetric sites relative to the side chains of different monomers within the same dimer, but at similar positions with respect to the side chains of monomers in different dimers.

Contacts between dimers. The side-to-side contacts between dimers are not extensive (Fig. 6). The interface primarily involves a region of well-ordered solvent molecules, as well as the extra-pore cesium ions, as described above. However, the regions between crystallographically related dimers in the direction along the helix axis are more well defined; the dimers stack up to form contiguous tubes, with each of the amino termini of one dimer abutting the carboxyl termini of an adjacent dimer. The dimers form a nearly continuous helix, because the orientations of the chains at the ends of the tubes are in register, almost as if there were an extra peptide bond holding together chains that are running in the same direction. The centers of the pores all line up in parallel. There are no direct hydrogen bonds between adjacent dimers, because the solvent molecules present at the entry to the pore produce a small displacement of the dimers relative to each other in the γ direction. Some ordered solvent molecules appear to act as bridges between carbonyl and amide groups in adjacent dimers.

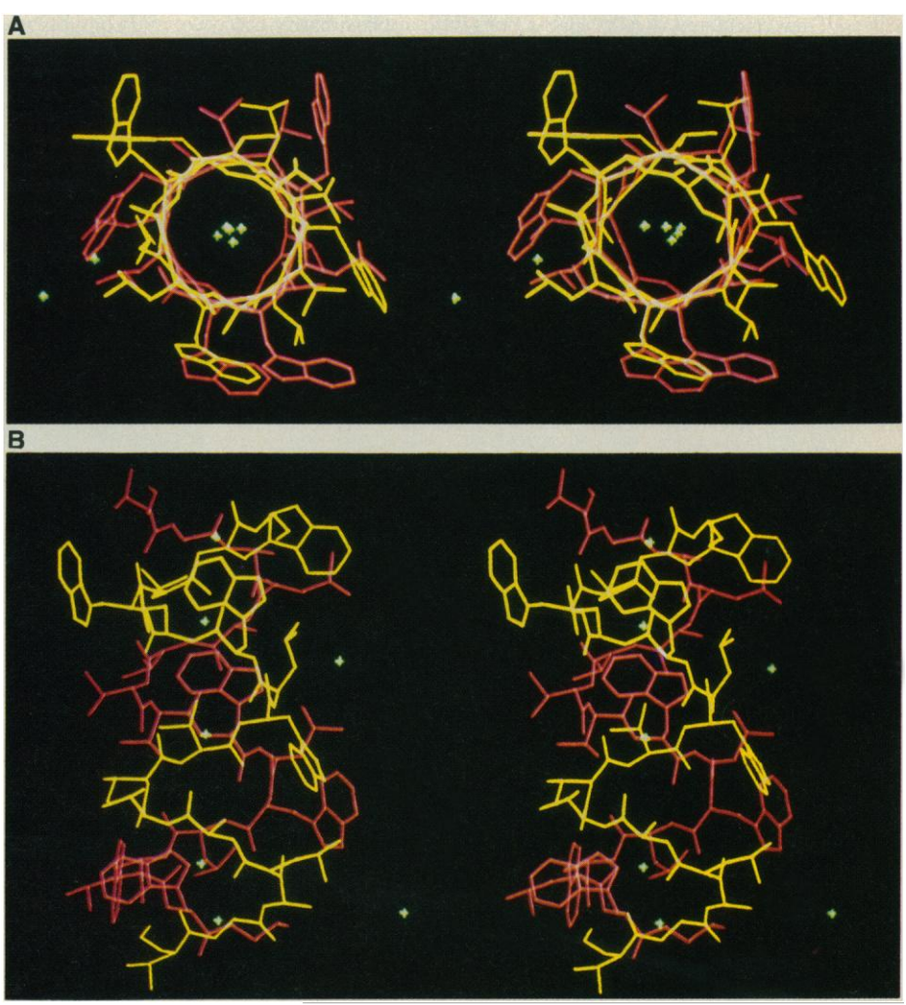

Fig. 4. (**A**) Stereographic view of one gramicidin dimer along the crystallographic *b* axis, corresponding to a view down the helix. The two polypeptide chains that comprise the dimeric pore are depicted in red and yellow. The cesium and chloride ion positions are indicated by (+). (**B**) Stereographic view perpendicular to (A) along the crystallographic *c* axis. The side chains form a hydrophobic exterior, whereas the peptide backbone forms a relatively hydrophilic pore that accommodates ions and solvent molecules.

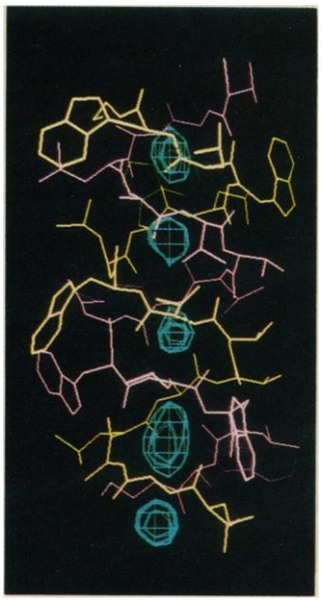

Fig. 5. Molecular structure showing the nature of the pore. The two different monomer chains are shown in red and yellow. The molecular model is superimposed on the highest contours of the electron density map (in blue), which are attributable to the cesium and chloride ions, in order to show the interaction of the ligands with the polypeptide backbone.

Comparisons with models proposed for the pore structure. The double helix motif for gramicidin was first proposed by Veatch *et al.* in 1974 (*8*). They suggested that either parallel or antiparallel helices with 7 residues per turn would be of the correct dimensions to form pores in black lipid membranes. Chandrasekaran and Prasad (*23*) then considered the stability of a number of antiparallel double helices. They calculated that favorable ones with approximately the correct dimensions would be those with either 5 or 7 residues per turn. They estimated the ϕ, ψ angles in the helix with 5 residues per turn to be -135, 140 and 160, -120 for L- and D-amino acids, respectively, and for the 7 residues per turn helix to be -135, 165 and 140, -140, respectively. Lotz *et al.* (*24*) used parameters from model L, D-compounds to propose double helices with 5.6 residues per turn and ϕ, ψ angles of -116, 141 and 159, -130; they also considered helices with 7.2 residues per turn, where the ϕ, ψ angles were -127, 146 and 154, -126. Koeppe and Kimura (*25*) developed a more detailed model for a double helical version of gramicidin with 5.8 residues per turn, which has a pitch of 11.2 Å. These various models have been used by a number of investigators for comparisons with experimental data on gramicidin in attempts to discriminate between the helical motifs present in different solvent environments (*26, 27*).

In the gramicidin-cesium crystal structure, each polypeptide chain actually has a pitch of 6.4 residues per turn, which differs from the pitches of all of the model double helical structures. The folding motif found in the pore structure has the same hydrogen-bonding pattern as proposed for the 7.2 residue models, but it has a different helical twist. Consequently, the average ϕ, ψ angles (-149, 114 and 84, -89 for the L- and D-amino acids, respectively) are quite different from those of any of the models. A major structural consequence of this is that the hydrogen bonds actually lie parallel to the helix axis, whereas in all of the models they are in the plane of the tube, but make angles with the helix axis of up to 30 degrees. This difference produces a significantly different orientation for the dipole moments relative to the pore axis, which may have important electrostatic ramifications. Hence, although structural models have been useful guides, the crystal structure exhibits a number of features that had not been predicted: the helical twist of the backbone, the side chain orientations, the presence of anions, the stagger of the polypeptide chains, and the irregularity (puckering) of the polypeptide backbone near the cation binding sites.

Structure-function relation. Functional properties of molecules are not always obvious from their crystal structures, but in the case of the gramicidin pore, it is clear how this polypeptide could act to transport ions across membranes. Although the gramicidin-cesium crystals have no phospholipid molecules present, we can envision that the hydrophobic and relatively uniform outer surface of the pore could permit efficient packing with the hydrophobic lipids in a bilayer and cause little distortion of the lipid fatty-acid chains in order to accommodate its relatively regular surface.

The pore is held together by 28 interchain hydrogen bonds, which could account for the stability of this dimeric form and for why it may form the conducting species with very long mean channel lifetimes compared with those found for the channel form (which is probably held together by only 6 interchain hydrogen bonds). That the pore corresponds to the minor conducting species is supported by studies on amino terminal–to–carboxyl terminal cross-linked dimers (*28*), and by studies of hybrid gramicidins with altered sequences (*29*). The steric constraints in the cross-linked dimers prevent them from forming channel structures, yet they form conducting species with properties similar to the less abundant single channels seen in black lipid film preparations containing native gramicidin. The hybrid channels consisting of chirally opposite constructions also cannot form helical dimer channels; they, too, form conducting species with very long mean channel lifetimes. As these structures have the same reversal potential as the channel form, this suggests they have a similar cation selectively.

What is not yet clear is why the channel form predominates over the pore form in membranes, since the pore has all the structural characteristics necessary, for a stable conducting species. Future comparisons between the pore and channel structures may clarify this and provide insight into how gramicidin interconverts between this structure. Recently, crystals of a gramicidin-lipid complex have been prepared and characterized (*13, 30*), and the solution of their structure should provide detailed information on the channel state.

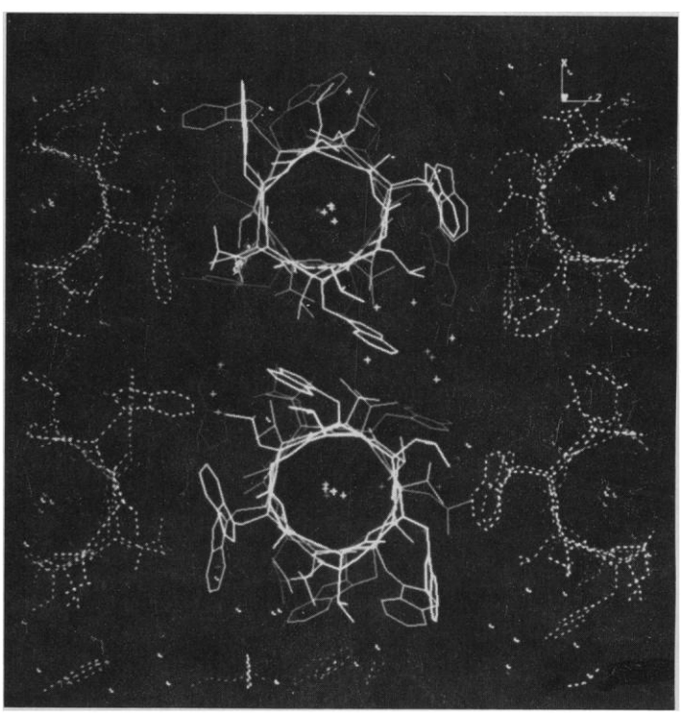

Fig. 6. The packing of gramicidin pores in the gramicidin-cesium crystal. In this view, along the crystallographic *b* axis, the two independent dimers in the asymmetric unit and their symmetry-related molecules are shown. The dimers form end-to-end stacks of tubes perpendicular to the plane of this figure.

One similarity between the two structures may be the residues that form the binding sites for the cations; although the binding sites in the pore are located at different positions relative to the ends of the tube compared with those in the channel, the residues involved (primarily Trp^{11} and Leu^{14}) appear to be those located near the ion binding sites in the channel form (*31*).

In summary, this structural analysis of the gramicidin-cesium complex has revealed the nature of ligand-polypeptide interactions in a solvent-filled ion pore. Such detailed structural information now provides a basis for studies of function and dynamics of this molecule, as well as for understanding its electrostatic interactions. Furthermore, the availability of data on both ion and solvent positions should be useful in future simulations of ion translocation in the pore.

REFERENCES AND NOTES

1. A. Finkelstein and O. S. Andersen, *J. Membr. Biol.* **59**, 155 (1981).
2. R. Sarges and B. Witkop, *J. Am. Chem. Soc.* **87**, 2011 (1965).
3. W. R. Veatch and L. Stryer, *J. Mol. Biol.* **113**, 89 (1977); W. R. Veatch, R. Mathies, M. Eisenberg, L. Stryer, *ibid.* **99**, 75 (1975).
4. D. W. Urry, M. C. Goodall, J. D. Glickson, D. F. Mayers, *Proc. Natl. Acad. Sci. U.S.A.* **68**, 672 (1971).
5. S. Weinstein, B. A. Wallace, J. S. Morrow, W. R. Veatch, *J. Mol. Biol.* **143**, 1 (1980).
6. L. T. Boni, A. J. Connolly, A. M. Kleinfeld, *Biophys. J.* **49**, 122 (1986).
7. E. Bamberg, H. J. Apell, H. Alpes, *Proc. Natl. Acad. Sci. U.S.A.* **74**, 2402 (1977).
8. W. R. Veatch, E. T. Fossel, E. R. Blout, *Biochemistry* **13**, 5249 (1974).
9. B. A. Wallace, *Biopolymers* **22**, 397 (1983).
10. ———, *Biophys. J.* **49**, 295 (1986).
11. D. C. Hodgkin, *Cold Spring Harbor Symp. Quant. Biol.* **14**, 65 (1949); R. L. M. Synge, *ibid.*, p. 191.
12. R. E. Koeppe, K. O. Hodgson, L. Stryer, *J. Mol. Biol.* **121**, 41 (1978); R. E. Koeppe, J. M. Berg, K. O. Hodgson, L. Stryer, *Nature* **279**, 723 (1979).
13. M. R. Kimball and B. A. Wallace, *Ann. N.Y. Acad. Sci.* **435**, 551 (1984).
14. B. Hedman, K. O. Hodgson, J. R. Helliwell, R. Liddington, M. Z. Papiz, *Proc. Natl. Acad. Sci. U.S.A.* **82**, 7604 (1985).
15. W. A. Hendrickson, J. L. Smith, S. Sheriff, *Methods Enzymol.* **115**, 41 (1985).
16. B. A. Wallace and W. A. Hendrickson, *Acta Cryst.* **A40**, c49 (1984).
17. ———, K. Ravikumar, in preparation.
18. W. A. Hendrickson and J. H. Konnert, *Computing in Crystallography*, R. Diamond, S. Ramasashan, K. Venkatesan, Eds. (Indian Academy of Sciences, Bangalore, 1980), p. 13.01.
19. T. A. Jones, *J. Appl. Cryst.* **11**, 268 (1978).
20. S. K. Burley and G. A. Petsko, *Science* **228**, 23 (1985).
21. G. Eisenman, J. P. Sandblom, E. Neher, *Biophys. J.* **22**, 307 (1978); *Metal-Ligand Interactions in Organic Chemistry and Biochemistry*, B. Pullman and N. Goldblum, Eds. (Reidel, Dordrecht, 1977), pp. 1–36.
22. S. Sung and P. C. Jordan, *Biophys. J.* **51**, 661 (1987).
23. R. Chandrasekaran and B. V. V. Prasad, *CRC Crit. Rev. Biochem.* (1978), pp. 125–161.
24. B. Lotz, F. Colonna-Cesari, F. Heitz, G. Spach, *J. Mol. Biol.* **106**, 915 (1976).
25. R. E. Koeppe and M. Kimura, *Biopolymers* **23**, 23 (1984).
26. V. M. Naik and S. Krimm, *Biophys. J.* **49**, 1131 (1986).
27. A. S. Arseniev, I. L. Barsukov, V. F. Bystrov, *FEBS Lett.* **180**, 33 (1985); ———, A. L. Lomize, Yu. A. Ovchinnikov, *ibid.* **186**, 168 (1985).
28. Yu. A. Ovchinnikov and V. T. Ivanov, in *Conformation in Biology*, R. Srinivasan and R. H. Sarma, Eds. (Adenine, Guilderland, NY, 1983), pp. 155–174; L. A. Fonina *et al.*, *Pept. Proc. Eur. Pept. Symp.* **16**, 469 (1981).
29. J. T. Durkin, O. S. Andersen, F. Heitz, Y. Trudelle, R. E. Koeppe, *Biophys. J.* **51**, 451a (1987).
30. B. A. Wallace, *J. Mol. Biol.*, in press.
31. D. W. Urry, K. U. Prasad, T. L. Trapane, *Proc. Natl. Acad. Sci. U.S.A.* **79**, 390 (1982).

32. We thank W. A. Hendrickson for helpful discussions and R. Murali for help in producing some of the figures. Supported by National Science Foundation grant DMB87-96207.

21 March 1988; accepted 18 May 1988